Pattern and Frequency Reconfigurable Annular Slot Antenna Using PIN Diodes

Symeon Nikolaou, Ramanan Bairavasubramanian, *Student Member, IEEE*, Cesar Lugo, Jr., *Student Member, IEEE*, Ileana Carrasquillo, Dane C. Thompson, *Student Member, IEEE*, George E. Ponchak, *Senior Member, IEEE*, John Papapolymerou, *Senior Member, IEEE*, and Manos M. Tentzeris, *Senior Member, IEEE*

***Abstract*—This paper presents the use of pin diodes to reconfigure the impedance match and modify the radiation pattern of an annular slot antenna (ASA). The planar antenna is fabricated on one side of a Duroid substrate and the microstrip feeding line with the matching network is fabricated on the opposite side of the board. The central frequency is 5.8 GHz and, by reconfiguring the matching circuit, the antenna was also designed to operate at 5.2 and 6.4 GHz. Pin diodes are also used to short the ASA in preselected positions along the circumference, thereby changing the direction of the null in the plane defined by the circular slot changes. As a proof of concept, two pin diodes are placed 45° on both sides of the feeding line along the ASA and the direction of the null is shown to align with the direction defined by the circular slot center and the diode. Consequently, a design that is reconfigurable in both frequency and radiation pattern is accomplished. Return loss and radiation pattern measurements and simulations are presented, which are in very good agreement.**

***Index Terms*—Annular slot antenna (ASA), frequency reconfigurability, pin diode, reconfigurable antenna, reconfigurable radiation pattern, slot antenna.**

I. Introduction

THE multitude of different standards in cell phones and other personal mobile devices require compact multi-band antennas and smart antennas with reconfigurable features. The use of the same antenna for different purposes, preferably in different frequencies is highly desirable. Moreover, as the number of users of the same spectrum increase, there is an increasing probability of interference between users. Thus, antennas with reconfigurable null positioning are critical. A number of different reconfigurable antennas, both planar and three–dimensional (3-D), have been developed for radar applications [1], [2] and wireless devices [3], [4]. Reconfigurable patch antennas were also designed to operate in both L and X bands [5]. Most of those papers demonstrate only frequency reconfigurability. The annular slot antenna (ASA) on dielectric material has been described explicitly in [6]. The effect of one shorted point along the circumference has been explored in [7], an application of a shorted ASA integrated with a narrowband filter is presented in [8], and the effect of capacitive loading is investigated in [9].

Manuscript received February 15, 2005; revised September 4, 2005. This work was supported in part by the Georgia Electronic Design Center and by the U.S. Army Research Office by Grant W911NF-04-1-0206.

S. Nikolaou, R. Bairavasubramanian, C. Lugo, Jr., I. Carrasquillo, D. C. Thompson, J. Papapolymerou, and M. M. Tentzeris are with the Georgia Institute of Technology, Atlanta, GA 30332 USA (e-mail: simos@ece.gatech.edu).

G. E. Ponchak is with NASA Glenn Research Center, Cleveland, OH 44135 USA (e-mail: george.ponchak@ieee.org).

Digital Object Identifier 10.1109/TAP.2005.863398

While the literature concerning the shorted ASA is limited, a significant number of papers have been published investigating feeding techniques and several antenna features like the input impedance, the radiation efficiency, and the radiation pattern of a pure ASA. For the antenna feature analysis, both analytical [10], [11] and numerical techniques [12] were used and different approaches or models were applied [13]. Various feeding lines [14] and feeding techniques are used in order to achieve broader bandwidth, or to demonstrate multiband operation [15]–[20]. In these designs all resonating frequencies are excited simultaneously. While the radiation pattern is an essential parameter of an antenna, very little has been published about radiation pattern control techniques for the ASA [21].

The reconfigurable ASA proposed in this paper operates at three frequencies with a central frequency at 5.8 GHz, and it also has a reconfigurable radiation pattern that can position a null within a 150° arc in the plane of the antenna. It is fabricated on low-cost material, utilizes high isolation, low-cost pin diodes, and is a compact design suitable for integrating in mobile systems. This is the first time an annular slot antenna with both frequency and radiation pattern reconfigurability is presented. For this antenna only one frequency resonates at a time, which is desirable when there are power or interference issues. Both simulations and experimental results of the return loss and radiation patterns are presented.

II. Theory of Operation

A. Design Concept

The annular slot antenna consists of a circular slot on a square, metal ground plane that is fed by a microstrip line fabricated on the opposite side of the substrate as can be seen in Fig. 1. The mean length of the slot circumference is approximately $3\lambda_s/2$ at the design frequency where λ_S is the equivalent wavelength in a slot transmission line with slot width w [22], which is small compared to λ_s. The microstrip feed line terminates in an open circuit that is approximately $\lambda_g/4$ from the ring where λ_g is the guided wavelength on the microstrip line. At the intersection of the microstrip line and the slot, magnetic coupling occurs, which, due to the $3\lambda_s/2$ ring circumference, creates a null in the radiation pattern in the direction of the microstrip feed line. In Fig. 1 and all subsequent figures *x*-*y* axes are used. The *x* axis corresponds to $\varphi = 0°$ and the *y* axis to the $\varphi = 90°$. The radiation patterns and all references on angle positions are consistent with the aforementioned notation. The radiation pattern and the null positioning are explained in detail in the theory section. To change the direction of the null, pin diodes are used to create short circuits

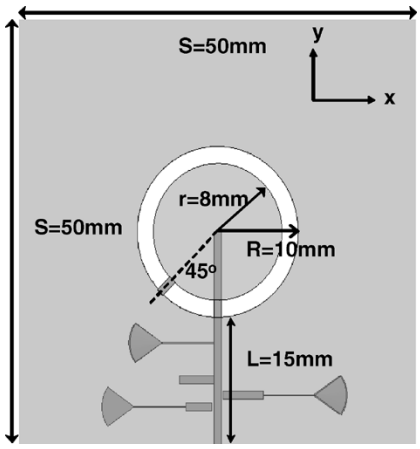

Fig. 1. Annular slot antenna schematic The feeding line with the matching stubs are on the bottom and the annular slot antenna is on the top side of the substrate. The short is placed at $\varphi = 225°$, else 45° far from the feeding line.

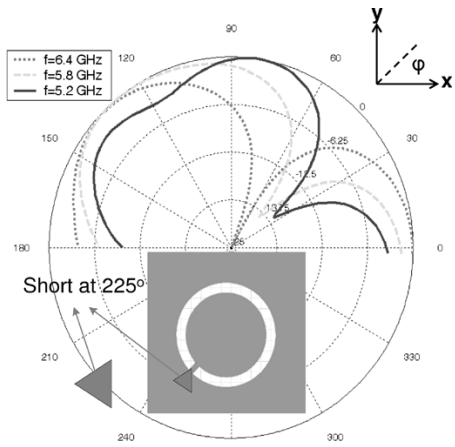

Fig. 2. Simulated normalized radiation patterns on the *x-y* plane with a short circuit at 225°. The null direction for the slot without any short would be in the 90° direction with respect to the plot labeling.

across the slot. Generally, a null appears opposite to the position where the short is placed, but the short position must be tuned to compensate for discontinuity in the slot fields caused by the feed line to achieve the desired null direction with accuracy. The simulation results indicate that a null can be created anywhere between 15° and 165° by adding a short in the opposite direction. For a nonreconfigurable design, the short circuits may be hard-wired slotline short circuits as shown in Fig. 1, but in the reconfigurable design, they are implemented with pin diodes. The short in the slot results in a reformation of the electric field distribution along the slot leading to a shift of the null in the short direction. It also changes the equivalent load at the input of the microstrip transmission line; therefore, reconfigurable matching stubs are required to keep the antenna matched at the design frequency during null reconfiguration. Linear matching stubs are also used to match the antenna at different frequencies when the slot configuration is kept constant. As a proof of concept, the antenna is designed to operate at 5.2 and 6.4 GHz in addition to the initial frequency of 5.8 GHz. To reconfigure the matching network, pin diodes are used to connect or disconnect the stubs from the microstrip transmission line and consequently shift the resonance to the desired frequency.

B. Pattern Reconfigurable Principles

The radiation patterns of the shorted ASA yield a null in a direction different than the feeding line direction, which is the case for the regular, unperturbed slot. The simulated *x-y* plane radiation patterns for the case of a hard-wired short circuit at 225° are presented in Fig. 2. In that plane the E field is polarized in φ direction, parallel to the slot plane. The null is created in the *x-y* plane instead of the broadside direction because it is meant to decrease the effect of an interferer coming from a direction different than the directivity (maximum field value) direction, which is parallel to z axis. At 5.8 GHz, for which the slot dimensions are optimized, a null exists exactly opposite to the slot short with respect to the slot center. At 6.4 GHz, the null appears approximately 10° closer to the 90° direction, while at 5.2 GHz, the null deviates from the 90° direction and moves closer to the 0° direction by 5°. Similarly, placing a short circuit at 315°, results in a null in the radiation pattern at 135° for 5.8 GHz. As a more general concept, when a frequency lower than the design frequency is used, the null shifts toward the $\varphi = 90°$ direction while it shifts toward the $\varphi = 0°$ direction when a higher frequency than the design frequency is used.

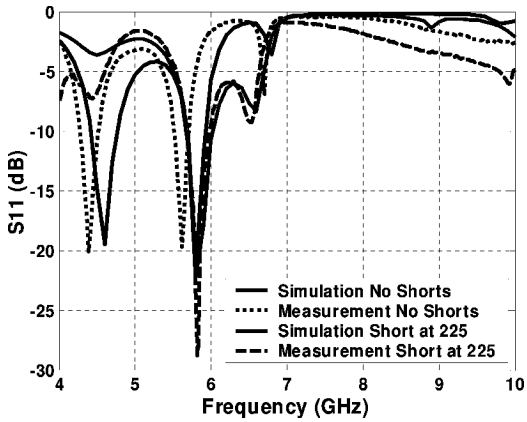

Fig. 3. Simulation and measurement results for the null reconfigurable design The first two lines refer to the design without any short. The numbers in the label refer to the hard-wired short position compared to the polar plot label in Fig. 2.

As discussed, varying the null position changes the impedance of the antenna and requires a reconfigurable matching circuit. When a short is placed at 45° from the feeding line, as shown in Fig. 1, a single stub with length 4.21 mm and width 0.92 mm at a distance of 7.27 mm from the feeding point is used to match this short position at 5.8 GHz. When the short is removed, simulating the case that the diode is not biased, a second stub must be added as a shunt matching device at the feeding line in order that the resonance frequency remains constant. The technique to define the stubs' length and their position is explained in the next section. Return loss simulation and measurements are presented in Fig. 3, where it is seen that a 5.8-GHz resonant frequency is maintained regardless whether or not a short exists. The 4.5-GHz parasitic resonance, when no short circuits occur on the ring, is easily removed by filtering it with a microstrip passband filter that can be cascaded to the antenna geometry.

To qualitatively explain the shift in the null direction when a short is placed along the slot, a novel but simple model using

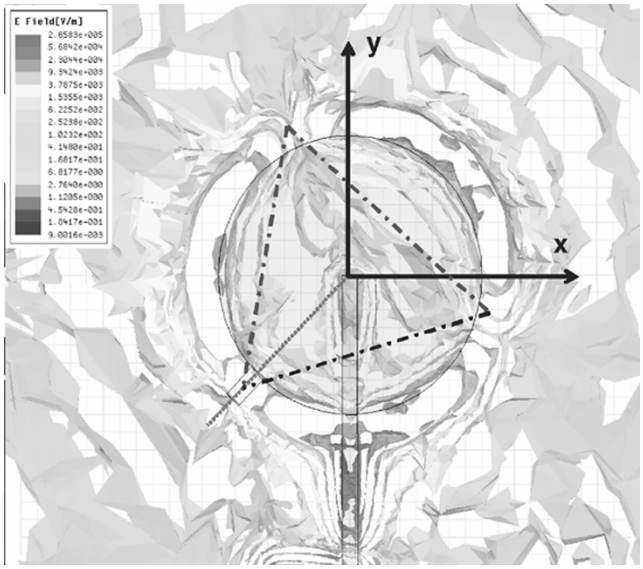

Fig. 4. Electric field distribution for f = 5.8 GHz when a short is placed at 225°. The dipoles model is superimposed for comparison.

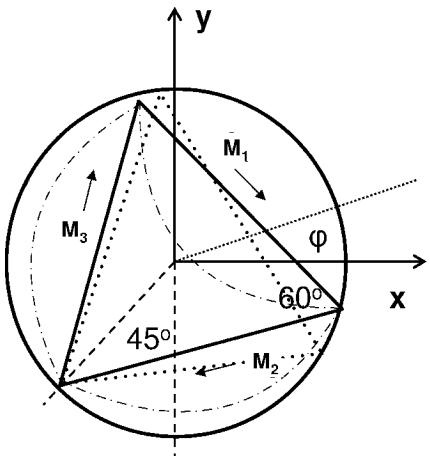

Fig. 5. Magnetic dipoles model of ASA with short circuit at 225°. Three dipoles are used in equilateral triangle orientation (Blue solid lines are for 5.8 GHz and green dotted lines for 5.2 GHz).

magnetic dipoles is introduced and briefly discussed. The field distribution as a result of a numerical simulation using HFSS [23] is presented in Fig. 4. Based on the field distribution, the dipole model presented in Fig. 5 is proposed, which consists of three magnetic dipoles of length $\lambda_s/2$ with sinusoidal magnetic current excitation. The $\lambda_s/2$ magnetic dipole is the dual equivalent to the $\lambda/2$ electric dipole. The electric field component E on a plane that includes an electric dipole with length l is given by [24]. Based on the duality principle [24] the E field derived from a magnetic dipole is presented in (1), where k is the wavenumber, r is the distance from the dipole's center, and M_o the amplitude of the magnetic current excitation. The angle θ is the elevation angle measured from the z axis which is parallel to the dipole. The dipoles for the proposed model lay on x-y plane, therefore, the azimuthal angle φ is used in (2) but the expression applied for each one dipole is still the expression in (1).

$$E(\theta) \simeq -j\frac{M_o e^{-jkr}}{2\pi r}\frac{\cos\left(\frac{kl}{2}\cos\theta\right)-\cos\left(\frac{kl}{2}\right)}{\sin\theta}. \quad (1)$$

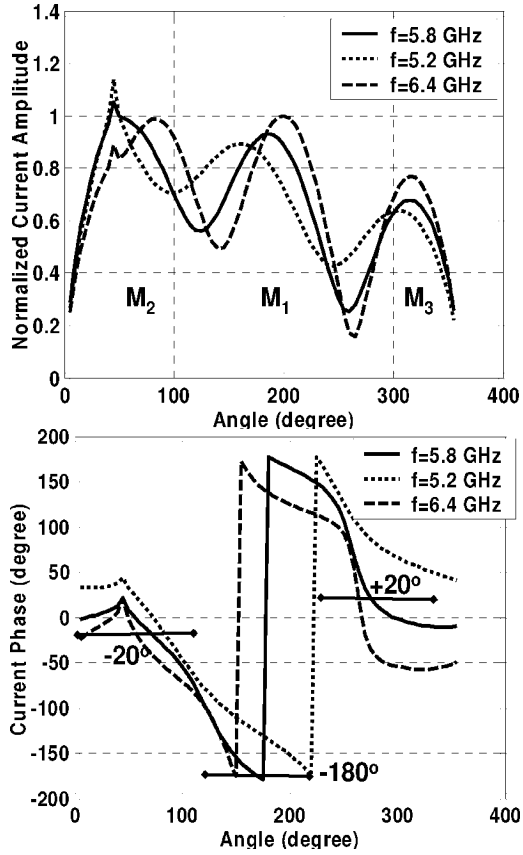

Fig. 6. (a) Magnetic current amplitude distribution along the annular slot. (b) Magnetic current phase distribution along the annular slot The 0 corresponds to the short position. The singularity at 45° is due the excitation source. The phases and normalized amplitudes correspond to M_2, M_1 and M_3 from left to the right.

The superimposed electric field as a result of all three dipoles is given by (2) and is plotted in Fig. 7 in polar coordinates.

$$E = \left| e^{j\delta_1}E_1\left(\phi+\frac{\pi}{4}\right) + e^{j\delta_2}e^{-jkd_2}E_2\left(\phi+\frac{\pi}{4}+\frac{2\pi}{3}\right) + e^{-j\delta_3}e^{-jkd_3}E_3\left(\phi+\frac{\pi}{4}-\frac{2\pi}{3}\right)\right|. \quad (2)$$

The phase shift $\pi/4$ is used to take into consideration the respective dipoles' orientation with respect to the reference axes. There is also a $2\pi/3$ angle between two consecutive dipoles which must be considered. In Fig. 6 the magnetic current and phase distribution along the annular slot, are presented as derived from the electric field distribution presented in Fig. 4. The magnetic current distribution presented in Fig. 6 matches the magnetic current distribution calculated and measured for the shorted annular slot, presented in [7].

For (2), the amplitude and phase for each magnetic current excitation must be estimated. The phases and amplitudes for the dipoles' currents for f = 5.8 GHz are calculated from the solid lines in Fig. 6 using the technique applied in [25]. The phases, δ_1, δ_2 and δ_3 are the phases of the current excitations and are calculated as the mean values of the continuous phase distribution in the corresponding segment, as shown in Fig. 6(b). Therefore from Fig. 6(b) the phases are estimated as $\delta_2 = -20°$,

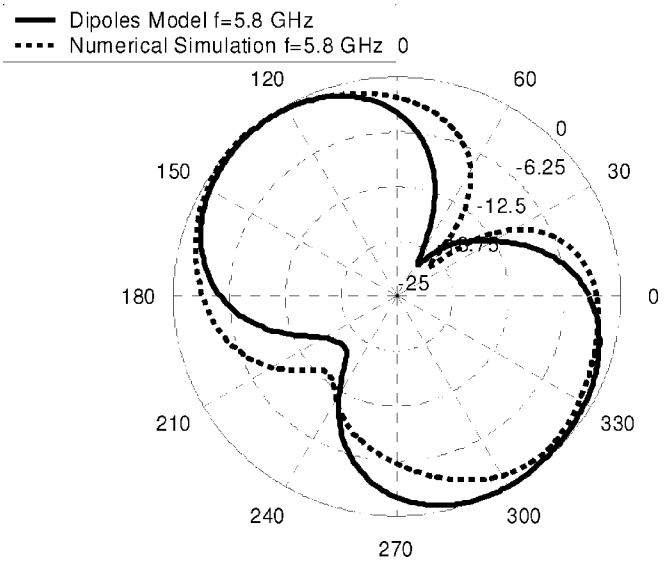

Fig. 7. Analytical expression plot of ASA with short circuit at 225° compared to the numerical solution for the amplitude of E field.

$\delta_1 = -180°$ and $\delta_3 = 20°$. The current amplitudes are normalized with respect to the strongest current M_2, which is the current on the segment where the excitation is applied. From Fig. 6(a) $M_1 = 0.9M_2$ and $M_3 = 0.7M_1$ are deduced. The amplitudes descent in that order, because of the traveling wave which is excited on the ring that attenuates as it propagates away from the excitation source. The path difference between E_1 and E_2, is $d_2 = (\lambda/4)\cos(60-\varphi)$ while the path difference between E_1 and E_3 is $d_3 = (\lambda/4)\cos(120-\varphi)$ and can be easily deduced geometrically. The normalized magnetic current excitations and the phases used, apply for any design frequency for which the annular slot length is $3\lambda_s/2$. The antenna prototype can be scaled for a different frequency without affecting the validity of the model.

The analytical model predicts the null position and matches the numerical solution with satisfactory precision as shown in Fig. 7 for the central frequency, $f = 5.8$ GHz. Measurements and the numerical solution show a shift in the null position as the frequency changes, which is predicted by the dipole model. At a different frequency, the slot circumference is no longer $3\lambda_s/2$ and a different field distribution occurs. As a result the magnetic dipoles do not maintain their orientation with respect to the axes, but they rotate slightly instead. For the lower frequency, the wavelength is about 10% longer and therefore the magnetic dipoles structure is rotated clockwise with the point at the short fixed. The current distribution for $f = 5.2$ GHz, for the dipole with M_2 excitation requires a longer segment along the ring [dotted line Fig. 6(a)] compared to the current 5.8 GHz. The $\lambda_s/2$ length at 5.2 GHz is about 10% longer than the one for 5.8 GHz so the dipoles structure is rotated clockwise with the point at the short fixed (dotted straight lines in Fig. 5). The dipole with currents M_1 and M_3 behave accordingly. The dipole with M_2 needs to be slightly shorter than $\lambda_s/2$ since it terminates at the short position and it overlaps with the feeding line. However it still remains close to $\lambda_s/2$. Therefore, the same analytical expression (2) is used with the offset angle to be slightly greater than $\pi/4$. That results in the rotation of the entire radiation pattern by the same offset angle clockwise as can be seen in Fig. 2. For the same reason, the use of a higher frequency at 6.4 GHz results a counter-clockwise rotation of the null direction. The proposed model aims primarily to give a qualitative explanation in the null shifting; therefore absolute agreement with the numerical solution should not be expected. The microstrip feed line and the matching circuits, which are only on one side of the ASA only, destroys the symmetry. Therefore the null is stronger in the direction opposite to the feeding line as can be seen in Fig. 7 where the simulation results in all 4 quadrants are presented.

C. Reconfigurable Matching Network

The ASA using various feeding techniques has been shown to have a relatively wide bandwidth compared to a patch or other narrowband antennas [26], [27]. For the design dimensions used in this paper, simulations predict radiation efficiency greater than 80% over the frequency range from 4.8 to 6.5 GHz. Since the radiating element can radiate over a wide range, the matching network must also support a broad bandwidth. Moreover, the use of diodes to create shorts in the annular ring for null reconfiguration also affects the input impedance, and this also must be accounted for in the matching circuit. Instead of a broadband matching network, a reconfigurable matching network employing stub tuners was designed to support three narrowband frequency ranges. At the center frequency of 5.8 GHz, the input admittance was determined from the simulations, and this admittance was transferred along the 50 Ω microstrip line to the point where the admittance had a real part of 0.02 siemens ($= 1/50$ siemens) and a random imaginary part. At that point, an open circuit microstrip stub was placed parallel to the transmission line to cancel the imaginary part. For the other frequencies, the impedance at the port needs to be determined with the first matching stub in place so the other two frequencies are matched using the combination of two stubs for each one of them. Those additional stubs have been shown not to affect in any way the radiation pattern. As an extension of section's (Section II-B) experiment for the validation of the frequency reconfigurability, the short on the slot is placed at 45° from the feeding line, namely at 225°. Because of symmetry, the same matching stubs can be used when the short is placed at the symmetrical position 45° toward the opposite direction, which is at 315°. In order to investigate the effect of the diodes, three different designs with the correct matching network hard wired for each of the three frequencies were tested. The return loss plots are presented in Fig. 8. Simulations and measurements are in good agreement, with a small shift downwards for the 6.4-GHz resonance, which could be a result of fabrication inaccuracy and imperfect connector soldering.

III. Antenna Design Description

A. Frequency Reconfigurable Design

A layout of the front side of the antenna with the matching stubs designed as described in Section II-C is presented in Fig. 9. For shorting and opening the stubs to the feeding line, ASI 8001 PIN diodes are used, which will be referred to as small diodes. Their length is less than 200 μm. On the annular slot, MBP-1035-E28 PIN diodes are used, which will be referred to as 'big'

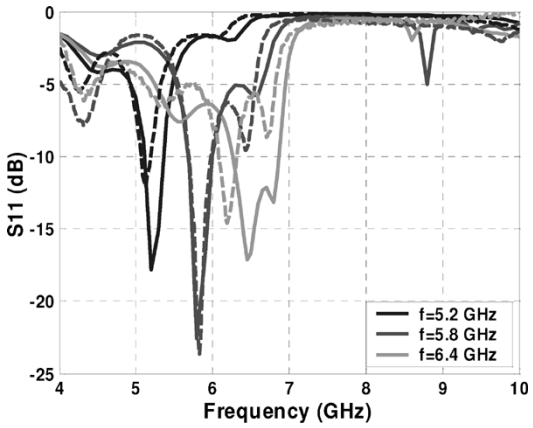

Fig. 8. Simulation and measurement are presented for the three different frequencies. Simulation is presented in solid line and measurement is presented in dashed line.

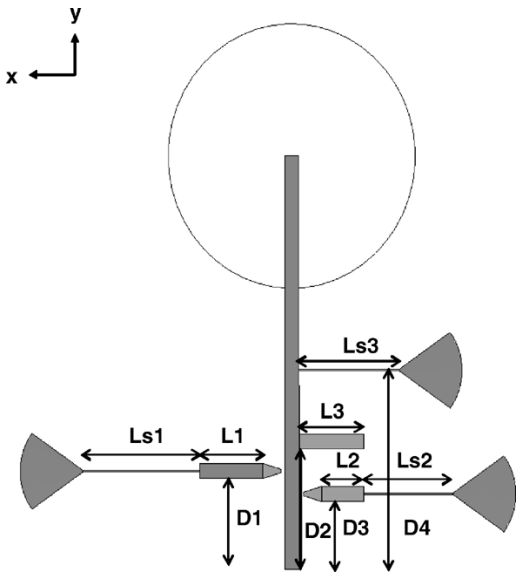

Fig. 9. ASA frequency reconfigurable design matching network.

diodes. They are long enough to cover the 2-mm slot width. The matching network for the frequency reconfigurable design with a "big" diode biased at 45° along the ASA is shown in Fig. 9. Three stubs of length L1, L3, and L2 are used to match the slot antenna to 5.2, 5.8, and at 6.4 GHz, respectively. The dc bias lines are used to apply the dc voltage to the small diodes. When neither of the small diodes is biased, the antenna is matched at 5.8 GHz, by forward biasing the diode on the stub of length L1, the antenna is matched at 5.2 GHz, and by forward biasing the diode on the stub of length L2, the antenna is matched to 6.4 GHz. The reconfigurable matching network dimensions are presented in Table I.

In Fig. 9, the 200 μm gaps (between the tapering small triangles and the feeding line) for the small diodes can be seen. The radial stubs are 70° wide and all the microstrip lines are 0.92 mm wide which results in a Zo of 50 Ω. The thin feeding lines are 120 μm wide and are used as dc bias lines. Their respective lengths are optimized for the frequency used, so they are equivalent to an open for the RF signal while they are perfect

TABLE I
DIMENSIONS OF CIRCUIT ELEMENTS FOR FREQUENCY RECONFIGURATION AND NULL AT 45°

Symbol	Value in mm
D1	5.49
D2	7.27
D3	4.10
D4	12.08
L1	4.05
L2	2.75
L3	4.21
Ls1	7.60
Ls2	5.75
Ls3	6.50

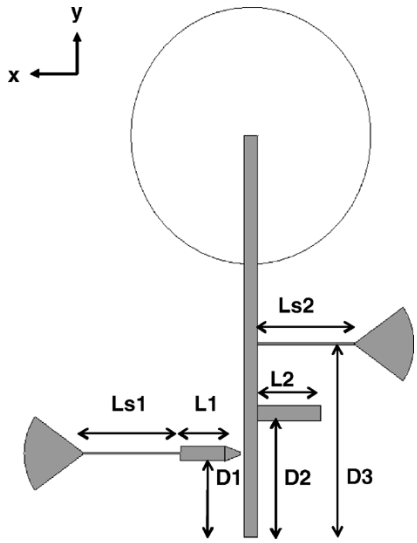

Fig. 10. ASA null reconfigurable design matching network.

conductors for any applied dc current. The dc lines however are thin enough (very high RF impedance) to prevent leakage for the frequencies for which they are not optimized. Tapered segments are used to match the wider linear stubs to the small diodes in order to minimize reflections.

B. Null Position Reconfigurable Design

For the null reconfigurable design, two stubs are used to match the antenna for the two cases; when there is a short at $\pm 45°$ away from the feeding line, and when no short exists along the circumference. Consequently one small diode is used for the activation of the matching stubs and two big diodes for the null control. When the small diode is not biased and one of the two big diodes is biased, the antenna is matched at 5.8 GHz. Note that this corresponds to the same matching network in Fig. 9. When none of the big diodes are biased and the small diode is biased, the antenna is matched at 5.8 GHz and a null appears in the direction opposite to the feeding line. As a result, for a fixed frequency at 5.8 GHz a null in three different directions ($-45°$, 0°, and $+45°$) can be created. The matching network design is presented in Fig. 10 and the dimensions are presented in Table II.

TABLE II
DIMENSIONS OF CIRCUIT ELEMENTS FOR NULL RECONFIGURATION AT 5.8 GHZ

Symbol	Value in mm
D1	4.75
D2	7.27
D3	12.08
L1	2.97
L2	4.21
Ls1	6.50
Ls2	6.50

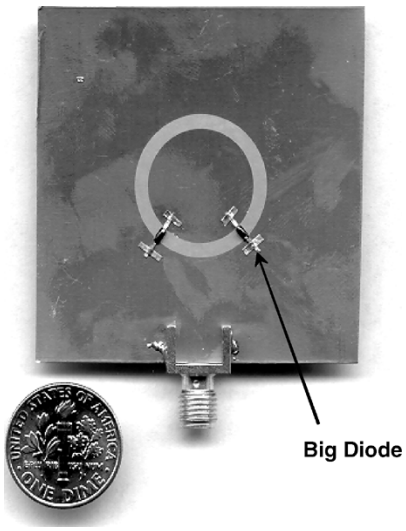

Fig. 11. Photograph of the front side of the annular slot antenna. Two MBP-1035-E28 PIN diodes are observed, soldered symmetrically 45 from the feeding line.

C. Fabrication

The antenna was fabricated on a 635-μm-thick Rogers RO3006 substrate with $\varepsilon_r = 6.15$ and $\tan\delta = 0.0025$. The antenna is fed by a 50-Ω microstrip line. A standard photolithography technique was used for fabrication. The copper thickness was 18 μm and the alignment between the two copper layers was achieved by drilling holes on the substrate using a laser method. Big and small diodes can be seen in Figs. 11 and 12, respectively. A current smaller than 10 mA, was used to forward bias the diodes. For the small diode bias, dc bias lines were used and a wire carrying the bias was soldered to the radial stub. For the big diodes, the ground plane was grounded and a wire was soldered to the inner section of the ring. For return loss and radiation pattern measurements a 3.5 mm SMA connector was soldered at the beginning of the feeding line.

IV. EXPERIMENTAL RESULTS DISCUSSION

A. Diodes' Effect in Return Loss

The small diodes are used to electrically connect the matching stubs to the transmission line. When the diodes are soldered onto the board but are not biased, they are equivalent to a small capacitive load (0.08 pF) and behave as if they do not exist for the frequencies of interest. That was verified in both return loss measurements and radiation pattern measurements. Return loss measurements to demonstrate the "small" diode effect are shown in Fig. 13.

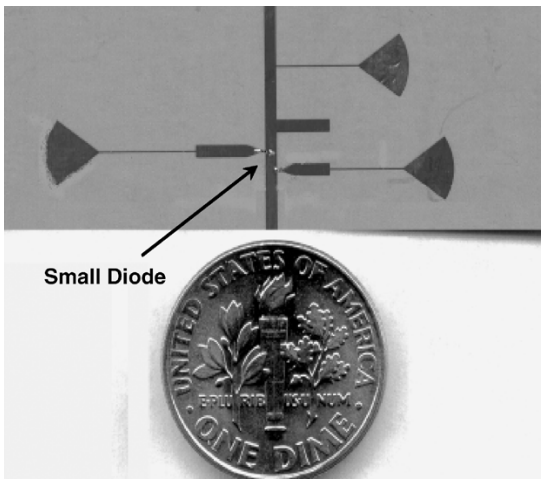

Fig. 12. Photograph of the back side of the frequency reconfigurable design. Two ASI 8001 PIN diodes are observed connecting the matching stubs to the feeding line. The dc bias lines are also visible.

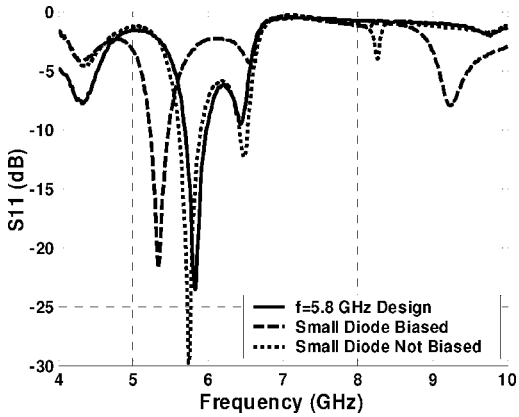

Fig. 13. Small diode effect in the frequency reconfigurable design for the 5.2-GHz stub.

When the diode is biased, the circuit is designed to match at 5.2 GHz, which is close to the measured resonant frequency in Fig. 13. When the diode is not biased, the antenna is designed to be matched at 5.8 GHz. The measurement with the diode not biased is compared to the reference hardwired design of Fig. 13 with no diodes on, and very good agreement is observed.

A small shift in the resonance frequency is consistently observed when a big diode is biased along the slot. The capacitive load on the circumference results in a downwards shift of the resonance frequency as discussed in [9]. For the null reconfigurable design, the coexistence of two diodes on the slot with one of them forward biased and the second one reverse biased results in a parasitic resonance close to 6.5 GHz, as seen in Fig. 14. This is because of the additional capacitive load as a result of the reverse biased diode. The parasitic resonance can be filtered with a cascaded microstrip passband filter for the single frequency (5.8 GHz) null reconfigurable antenna. For the extension to multiple frequencies, the parasitic will be taken care of with the appropriate matching configuration. For the simulation, the reverse biased diode was simulated as a perfect open and that is why the parasitic resonance does not appear in the simulation. There

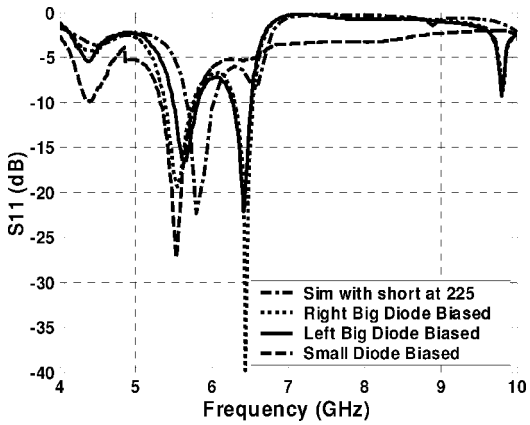

Fig. 14. Diodes effect in return loss measurement for the null reconfigurable design. The design frequency was 5.8 GHz.

is still a good resonance at the design frequency which is consistent for all three directions of the null and is measured at 5.65 GHz which is less than 3% off the design frequency.

B. Radiation Pattern Measurement

A far field antenna test range was used to characterize the ASA. In the test range, the ASA was the receiving antenna that rotated through the ϕ plane while a 5.4–8.2 GHz, 15-dB standard gain horn was used as the fixed, transmitting antenna; the two antennas were separated by 1 m. The transmitted RF signal was AM modulated by a 20-MHz signal that was detected by a diode detector and measured by a lock-in amplifier. Control of the rotary stage, lock-in amplifier, and data recording was automated. To bias the diodes, wires were soldered to the center of the ASA and the radial stubs of the matching circuit. In addition, a bias tee was used to ground the microstrip line and to isolate the applied bias from the diode detector. Because the ASA radiates backward as well as forward, the coaxial launcher, bias tee, and detector were sandwiched between 1-cm-thick pieces of absorbing material. During test, it was observed that the substrate corners had to be rounded to minimize reflections and diffractions at the corners that caused ripples in the radiation pattern. Before characterizing the ASA, a variable attenuator was used to vary the input power in order to calibrate the diode detector and determine the radiated power that results in maximum detector sensitivity.

C. Diodes Effect in Radiation Pattern

The effect of both the small and big diodes on the radiation patterns was investigated and is presented in the current section, and the radiation patterns are compared to the simulation results (ideal elements) and to the hard-wired design measurements presented earlier. In Fig. 15, the measured radiation patterns for the E_φ component of the electric field, which is the component parallel to the antenna substrate, for all three frequencies and a hardwire short at 225° are shown, In addition, the measured radiation pattern at 5.2 GHz for a regular slot without any short along the slot is shown. The results in Fig. 15 have similar behavior to the simulated results presented in Fig. 2 in Section II. The shift in the null direction with respect to the frequency that was explained in a previous section is hereby verified experimentally.

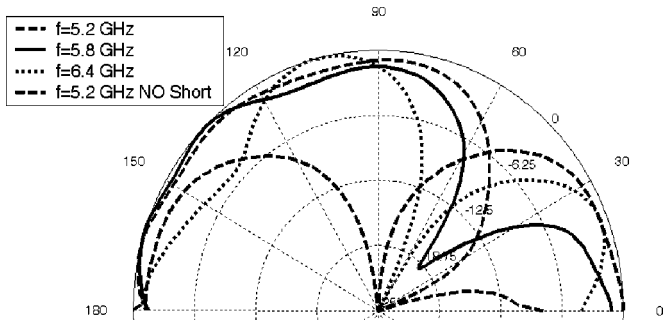

Fig. 15. Measured radiation patterns for the design frequencies when a hard-wired short is placed at 225°.

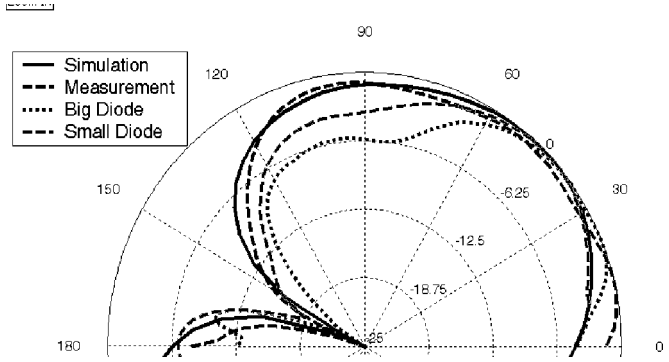

Fig. 16. Radiation patterns for the 5.2-GHz frequency design when the short is placed at 315°. Simulation, measurement with hard-wired short, measurement with the big diode biased, and measurement with the small diode biased are presented.

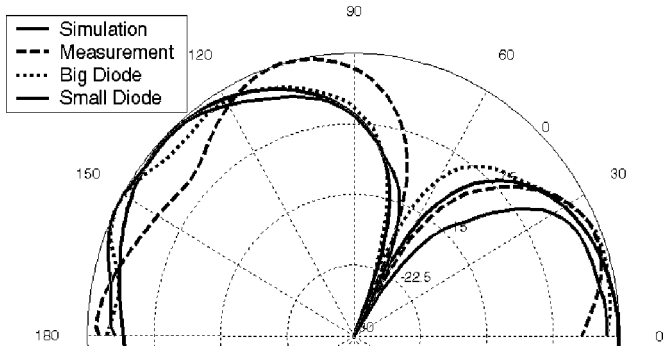

Fig. 17. Radiation patterns for the 6.4-GHz frequency design when the short is placed at 225°. Simulation, measurement with hard-wired short, measurement with the big diode biased, and measurement with the small diode biased are presented.

Figs. 16 and 17 present the measured radiation patterns for frequencies of 5.2 and 6.4 GHz, respectively, with diodes used to short the slot. They were in very good agreement with the simulation and the hard-wired measurements. This proves that the PIN diode is a suitable switch for this application. The effectiveness of the small diodes has been verified in designs other than antennas, like filters [28] and it only has to do with the matching network. The parasitic capacitance and resistive load of the big diodes that differentiate them from the ideal short circuit, on the other hand, have been hereby proven experimentally not to distort the radiation pattern in comparison to the ideal elements.

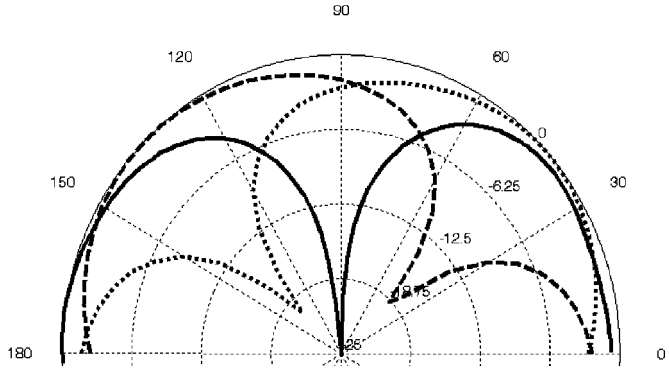

Fig. 18. Simulated radiation patterns in x-y plane for the null reconfigurable design at $f = 5.8$ GHz. The null is directed at 45°, 90°, and 135° direction. The 90° direction is the null direction when no short is used.

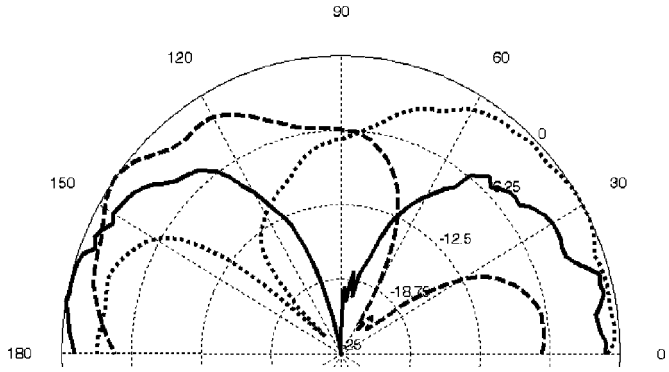

Fig. 19. Measured radiation patterns in x-y plane for the null reconfigurable design at $f = 5.65$ GHz. The null is directed at 45°, 90°, and 135° direction using two PIN diodes placed at. 225° and 315°.The 90° direction is achieved when none of the diodes is biased.

The short was placed in symmetrical positions with respect to the feeding line direction in order to show that the results are not dependent on the side of the short and are not affected from the non symmetric matching stubs. The behavior of the antenna is equivalent for both sides of the short.

In the plots presented in Figs. 16 and 17, the measurements were taken for different samples in order to compare and evaluate the effect of small and big diodes independently. For the null reconfigurable design (Figs. 18 and 19) all measurements were taken for the same sample on which three diodes are used and biased individually to steer the null in the three directions and maintain a constant resonant frequency. In order to get the nulls in the side directions, the corresponding big diode is biased. In order to get the null in the feeding line direction, the small diode on the matching stub L1 in Fig. 10 is biased in order to maintain the resonance frequency constant at 5.65 GHz while none of the big diodes is biased. In Figs. 18 and 19 where the simulated and measured results are presented, respectively, it is obvious that the steering of the null is achieved with high precision. The slot dimensions are optimized for the frequency of 5.8 GHz and for that frequency the null is exactly at 45° off the feed line direction. The measured patterns are for $f = 5.65$ GHz which is very close to the design frequency and as a result the null directions verify the simulation with high accuracy. In the 90° direction the simulated field is stronger than the measurement but overall good agreement is demonstrated.

V. Conclusion

A new design for both pattern and frequency reconfigurable annular slot antenna was presented. Matching stubs are used to match the antenna to three different frequencies, 5.2 and 6.4 GHz in addition to the initial central frequency at 5.8 GHz. PIN diodes are used to connect or disconnect the stubs creating a reconfigurable matching network. The radiation pattern control is achieved by activating/deactivating shorts on the slot. As a result the null is redirected to a different direction. As a benchmarking approach, the shorts are implemented by use of pin diodes. When each diode is forward biased, it is equivalent to a short, and when it is reverse biased, it behaves as a capacitive load. In the latter case, when no diodes are forward biased, the slot antenna behaves like the unloaded slot antenna and the null appears in the feeding line direction. The results for this antenna are presented at three separate frequencies. Any other frequency can be matched using the same technique as long as the radiation efficiency for that frequency is satisfactory. The same applies with the position of the shorts. The possible directions are not limited to the ones used in this paper but in that case also, the matching stubs need to be redesigned and optimized for the preferred short direction, since the short direction affects the equivalent load at the end of the transmission line. The measured results are compared to the simulations and are found to be in very good agreement. The proposed antenna is compact and easy to integrate with other microwave components. This antenna is the first step toward more mature compact reconfigurable slot antennas both in frequency and radiation pattern using pin diodes or RF MEMS switches.

Acknowledgment

The authors would like to acknowledge Dr. R. Li's assistance.

References

[1] J. T. Bernhard, R. Wang, R. Clark, and P. Mayes, "Stacked reconfigurable antenna elements for space-based radar applications," in *IEEE Antennas and Propagation Society Int. Symp.*, vol. 1, Jul. 2001, pp. 158–161.

[2] K. Tomiyasu, "Conceptual reconfigurable antenna for 35 GHz high-resolution spaceborne synthetic aperture radar," *IEEE Trans. Aerosp. Electron. Syst.*, vol. 39, pp. 1069–1074, Jul. 2003.

[3] J. T. Aberle, S.-H. Oh, D. T. Auckland, and S. D. Rogers, "Reconfigurable antennas for wireless devices," *IEEE Antennas Propag. Mag.*, vol. 45, no. 6, pp. 148–154, Dec. 2003.

[4] G. H. Huff, J. Feng, S. Zhang, G. Cung, and J. T. Bernhard, "Directional reconfigurable antennas on laptop computers: Simulation, measurement and evaluation of candidate integration positions," *IEEE Trans. Antennas Propag.*, vol. 52, pp. 3220–3227, Dec. 2004.

[5] W. H. Weedon, W. J. Payne, and G. M. Rebeiz, "MEMS-switched reconfigurable antennas," in *IEEE Antennas and Propagation Society Int. Symp.*, vol. 3, Jul. 2001, pp. 654–657.

[6] C. E. Tong and R. Blundel, "An annular slot antenna on a dielectric half-space," *IEEE Trans. Antennas Propag.*, vol. 2, pp. 967–974, Jul. 1994.

[7] H. Morishita, K. Hirasawa, and K. Fujimoto, "Analysis of a cavity-backed annular slot antenna with one point shorted," *IEEE Trans. Antennas Propag.*, vol. 39, pp. 1472–1478, Oct. 1991.

[8] S. Kanamaluru, M.-Y. Li, and K. Chang, "Narrowband filter and annular slot antenna for PCS applications," in *IEEE MTT-S Int. Microwave Symp. Dig.*, vol. 2, Jun. 1996, pp. 987–990.

[9] C.-S. Hong, "Small annular slot antenna with capacitor loading," *Electron. Lett.*, vol. 36, no. 2, pp. 110–111, Jan. 2000.

[10] K. Prasad and L. Shafai, "'Higher order mode excitation in circular loop and annular slot antennas," in *IEEE Antennas and Propagation Soc. Int. Symp.*, vol. 25, Jun. 1987, pp. 824–827.

[11] P. Mastin, B. Rawat, and M. Williamson, "Design of a microstrip annular slot antenna for mobile communications," in *IEEE Antennas and Propagation Society Int. Symp. Dig. Held in Conjuction with: URSI Radio Science Meeting and Nuclear EMP Meeting*, vol. 1, Jul. 1992, pp. 507–510.
[12] E. Irzinski, "The input admittance of a TEM excited annular slot antenna," *IEEE Trans. Antennas Propag.*, vol. 23, pp. 829–834, Nov. 1975.
[13] N. Nikolic, J. S. Kot, and T. S. Bird, "Theoretical and experimental study of a cavity-backed annular-slot antenna," *Inst. Elect. Eng. Proc. Microwaves, Antennas and Propag.*, vol. 144, no. 5, pp. 337–340, Oct. 1997.
[14] M.-H. Yeh, P. Hsu, and J.-F. Kiang, "Analysis of a CPW-fed slot ring antenna," in *Asia-Pacific Microwave Conf.*, vol. 3, Dec. 2001, pp. 1267–1270.
[15] P. Minard and A. Louzir, "A new wide frequency band feeding technique of annular slot antenna," in *IEEE Antennas and Propagation Soc. Int. Symp.*, vol. 1, Jun. 2002, pp. 406–409.
[16] H. Tehrani and K. Chang, "A multi-frequency microstrip-fed annular slot antenna," in *IEEE Antennas and Propagation Soc. Int. Symp.*, vol. 2, Jul. 2000, pp. 632–635.
[17] F. Le Bolter and A. Louzir, "Multi-band annular slot antenna for WLAN applications," in *IEEE Antennas and Propagation Soc. Conf.*, vol. 2, Apr. 2001, pp. 529–532.
[18] Q. Li, Z. Shen, and X. Shan, "A new microstrip-fed cavity-backed annular slot antenna," in *IEEE Antennas and Propagation Soc. Int. Symp.*, vol. 3, Jun. 2002, p. 68.
[19] Y. H. Suh and I. Park, "A broadband eccentric annular slot antenna," in *IEEE Antennas and Propagation Soc. Int. Symp.*, vol. 1, Jul. 2001, pp. 94–97.
[20] N. Behdad and K. Sarabandi, "A wideband bi-semicircular slot antenna," in *IEEE Antennas and Propagation Soc. Symp.*, vol. 2, Jun. 2004, pp. 1903–1906.
[21] P. R. Urwin-Wright, G. S. Hilton, I. J. Craddock, and P. N. Fletcher, "An electrically-small annular slot operating in the 'DC' mode," in *12th Int. Conf. Antennas and Propagation*, vol. 2, Apr. 2003, pp. 686–689.
[22] K. C. Gupta, R. Garg, I. Bah, and P. Bhartia, *Microstrip Lines and Slotlines*, Second ed. Norwood, MA: Artech House, pp. 282–286.
[23] Ansoft HFSS.
[24] C. A. Balanis, *Antenna Theory Analysis and Design*, Second ed. New York: Wiley, pp. 152–157.
[25] R. L. Li, V. F. Fusco, and R. Cahil, "Pattern shaping using a reactively loaded wire loop antenna," *Inst. Elect. Eng. Proc. Microwaves, Antennas and Propag.*, vol. 148, no. 3, pp. 203–208, Jun. 2004.
[26] P. Hallbjorner, "Electrically small unbalanced four-arm wire antenna," *IEEE Trans. Antennas Propag.*, vol. 52, pp. 1424–1428, Jun. 2004.
[27] R. Li, G. DeJean, M. M. Tentzeris, and J. Laskar, "Development and analysis of a folded shorted-patch antenna with reduced size," *IEEE Trans. Antennas Propag.*, vol. 52, pp. 555–562, Feb. 2004.
[28] C. Lugo and J. Papapolymerou, "Electronic switchable bandpass filter using PIN diodes for wireless low cost system-on-a-package applications," *Inst. Elect. Eng. Proc. Microwaves, Antennas and Propag.*, vol. 151, no. 6, pp. 497–502, Dec. 2004.

Symeon Nikolaou received the Diploma in electrical and computer engineering from the National Technical University of Athens (NTUA), Greece, in 2003.

He is currently pursuing the Ph.D. degree in electrical engineering with the Georgia Institute of Technology, Atlanta. His current research interests include the design and development of compact UWB and reconfigurable antennas, and RF packaging and design

Ramanan Bairavasubramanian (S'03) received the B.E. (EEE) degree from Anna University, Chennai, India, in May 2001 and the M.S.E.E. degree from the Georgia Institute of Technology, Atlanta, in December 2002.

He is currently pursuing the Ph.D. degree in electrical engineering at the Georgia Institute of Technology. His research interests include development of reconfigurable phased antenna arrays on multilayer LCP technology, as well as design and fabrication of compact RF filters and passives on organic substrates.

Cesar Lugo, Jr. (S'01) received the B.S. and M.S. degree in electrical engineering from the Georgia Institute of Technology (Georgia Tech), Atlanta, in 2002 and 2003, respectively.

He is currently working toward the Ph.D. degree in electrical engineering at Georgia Tech. He is with the MircTech group where his research consists of developing design techniques for reconfigurable RF/millimeter-wave filters and other components such as antennas, couplers, and tuners. Other research interests include advanced synthesis techniques for asymmetrical planar filters and dual-mode topologies.

Ileana Carrasquillo, photograph and biography not available at the time of publication.

Dane C. Thompson (S'98) was born in Sacramento, CA, in February 1979. He received the B.S. and M.S. degrees in electrical engineering from Santa Clara University, Santa Clara, CA, in 2001 and 2002, respectively.

He is currently working toward the Ph.D. degree in electrical and computer engineering at the Georgia Institute of Technology, Atlanta. His research involves the processing and use of LCP as a high-performance dielectric substrate and packaging material. He is currently researching the utilization of LCP for vertically integrated RF front-ends, for MMIC and MEMS packaging, and for dual-frequency dual-polarization multilayer conformal antennas

George E. Ponchak (S'82–M'83–SM'97) received the B.E.E. degree from Cleveland State University, Cleveland, OH, in 1983, the M.S.E.E. degree from Case Western Reserve University, Cleveland, in 1987, and the Ph.D. degree in electrical engineering from the University of Michigan, Ann Arbor, in 1997.

He joined the Communication Technology Division, NASA Glenn Research Center, Cleveland, in 1983 where he is now a Senior Research Engineer. During 1997–1998 and 2000–2001, he was a visiting lecturer at Case Western Reserve University. He has authored and coauthored 115 papers in refereed journals and symposia proceedings. His research interests include the development and characterization of microwave and millimeter-wave printed transmission lines and passive circuits, multilayer interconnects, uniplanar circuits, Si and SiC radio frequency integrated circuits, and microwave packaging.

Dr. Ponchak is a senior member of the IEEE Microwave Theory and Techniques Society (MTT-S), a member of the International Microelectronics and Packaging Society (IMAPS), and an Associate Member of the European Microwave Association. He was Editor of a special issue on Si MMICs in the IEEE TRANSACTIONS ON MICROWAVE THEORY AND TECHNIQUES. He founded the IEEE Topical Meeting on Silicon Monolithic Integrated Circuits in RF Systems and served as its Chair in 1998, 2001, and 2006 and was its Digest Editor in 2000 and 2003. He founded the Cleveland MTT-S/AP-S Chapter and serves as its Chair. He has chaired many MTT-S International Microwave Symposium workshops and special sessions. He is a member of the IEEE International Microwave Symposium Technical Program Committee on Transmission Line Elements and served as its Chair in 2003–2005, a member of IEEE MTT-S AdCom Membership Services Committee, and a member of the IEEE MTT-S Technical Committee 12 on Microwave and Millimeter-Wave Packaging and Manufacturing. He received the Best Paper of the ISHM'97 30th International Symposium on Microelectronics Award.

John Papapolymerou (S'90–M'99–SM'04) received the B.S.E.E. degree from the National Technical University of Athens, Athens, Greece, in 1993, and the M.S.E.E. and Ph.D. degrees from the University of Michigan, Ann Arbor, in 1994 and 1999, respectively.

From 1999 to 2001, he was a faculty member with the Department of Electrical and Computer Engineering, University of Arizona, Tucson, and during the summer of 2000 and 2003 he was a visiting professor with The University of Limoges, France. From 2001 to 2005, he was an Assistant Professor with the School of Electrical and Computer Engineering, Georgia Institute of Technology, where he is currently an Associate Professor. His research interests include the implementation of micromachining techniques and MEMS devices in microwave, millimeter-wave and THz circuits, and the development of both passive and active planar circuits on semiconductor (Si/SiGe, GaAs) and organic substrates (LCP, LTCC) for system-on-a-chip (SOC)/ system-on-a-package (SOP) RF front ends. He has authored or coauthored over 120 publications in peer reviewed journals and conferences.

Dr. Papapolymerou received the 2004 Army Research Office (ARO) Young Investigator Award, the 2002 National Science Foundation (NSF) CAREER award, the Best Paper Award at the 3rd IEEE International Conference on Microwave and Millimeter-Wave Technology (ICMMT2002), Beijing, China, and the 1997 Outstanding Graduate Student Instructional Assistant Award presented by the American Society for Engineering Education (ASEE), The University of Michigan Chapter. His student also received the Best Student Paper Award at the 2004 IEEE Topical Meeting on Silicon Monolithic Integrated Circuits in RF Systems, Atlanta, GA. He currently serves as the Vice-Chair for Commission D of the US National Committee of URSI and as an Associate Editor for the IEEE TRANSACTIONS ON ANTENNAS AND PROPAGATION. During 2004, he was the Chair of the IEEE MTT/AP Atlanta Chapter.

Manos M. Tentzeris (S'89–M'98–SM'03) received the diploma degree in electrical and computer engineering from the National Technical University of Athens, Greece, and the M.S. and Ph.D. degrees in electrical engineering and computer science from the University of Michigan, Ann Arbor.

He is currently an Associate Professor with the School of ECE, Georgia Institute of Technology, Atlanta. He has helped develop academic programs in highly integrated/multilayer packaging for RF and wireless applications, microwave MEM', SOP-integrated antennas, RF IDs 3D integration, and adaptive numerical electromagnetics (FDTD, MultiResolution Algorithms) and heads the ATHENA research group (15 researchers). He is the Georgia Tech NSF-Packaging Research Center Associate Director for RF Research and the RF Alliance Leader. He is also the leader of the Novel Integration Techniques Subthrust of the Broadband Hardware Access Thrust of the Georgia Electronic Design Center (GEDC) of the State of Georgia. He has published more than 200 papers in refereed journals and conference proceedings and eight book chapters. He is also in the process of writing two books.

Dr. Tentzeris was the recipient of the 2006 IEEE MTT Outstanding Young Engineer Award, the 2004 IEEE TRANSACTIONS ON ADVANCED PACKAGING Commendable Paper Award, the 2003 NASA Godfrey "Art" Anzic Collaborative Distinguished Publication Award for his activities in the area of finite-ground low-loss low-crosstalk coplanar waveguides, and the the 2003 IBC International Educator of the Year Award. He also received the 2003 IEEE CPMT Outstanding Young Engineer Award for his work on 3-D multilayer integrated RF modules, the 2002 International Conference on Microwave and Millimeter-Wave Technology Best Paper Award (Beijing, China) for his work on Compact/SOP-integrated RF components for low-cost high-performance wireless front-ends, the 2002 Georgia Tech-ECE Outstanding Junior Faculty Award, the 2001 ACES Conference Best Paper Award, and the 2000 NSF CAREER Award for his work on the development of MRTD technique that allows for the system-level simulation of RF integrated modules. He received the 1997 Best Paper Award of the International Hybrid Microelectronics and Packaging Society for the development of design rules for low-crosstalk finite-ground embedded transmission lines. He was also the 1999 Technical Program Co-Chair of the 54th ARFTG Conference, Atlanta. He is the Vice-Chair of the RF Technical Committee (TC16) of the IEEE CPMT Society. He has organized various sessions and workshops on RF/Wireless Packaging and Integration in IEEE ECTC, IMS, and APS Symposia in all of which he is a member of the Technical Program Committee in the area of "Components and RF." He was a Visiting Professor with the Technical University of Munich, Germany, for the summer 2002, where he introduced a course in the area of high-frequency packaging. He has given more than 40 invited talks in the same area to various universities and companies in Europe, Asia, and America. He is a member of URSI-Commission D, an Associate Member of EuMA, and a member of the Technical Chamber of Greece.